JOURNAL OF OPTOELECTRONICS AND ADVANCED MATERIALS Vol. 10, No. 1, January 2008, p. 124 - 130

Photoinduced anisotropic deformations in covalent chalcogenide glasses

K. TANAKA*, N. TERAKADO, A. SAITOH
Department of Applied Physics, Graduate School of Engineering, Hokkaido University, Sapporo, 060-8628, Japan

The chalcogenide glass is known to exhibit prominent anisotropic deformations when illuminated by linearly-polarized bandgap light. We report new deformation phenomena for As_2S_3. We also propose that many deformation phenomena can be accounted for by an optical force model.

(Received January 4, 2008; accepted January 10, 2008)

Keywords: Chalcogenide glass, Photoinduced deformation, Anisotropy, Opto-mechanical, Optical torque, Birefringence, Fluidity

1. Introduction

Recent studies have demonstrated that light illumination can produce prominent deformations in soft materials such as chalcogenide glasses and azo-polymers [1-5]. Deformations induced by unpolarized (or circularly polarized) and linearly polarized light are isotropic [1,2] and anisotropic [3-5], respectively, which are sometimes referred to as scalar and vector phenomena. Several observations suggest that, in these deformations, light-induced temperature rises can be neglected; *i.e.*, the phenomena occur athermally. However, underlying photo-structural mechanisms are largely speculative. In most cases, some photo-electro-atomic processes have been assumed [1-5] and simulated [6,7], but final elucidations remain. By contrast, in a recent work [8], Tanaka has proposed an optical force model, not atomic, for interpretation of a visible anisotropic deformation of glassy As_2S_3 flakes.

In the present work, we report new photoinduced deformation phenomena in As_2S_3 ($E_g \approx 2.4$ eV) with a brief review of the vector deformation in chalcogenide glasses. We also see that many of these phenomena can be accounted for in a coherent way using the optical force model. The idea will be valuable for understanding light-matter interactions and also for developing new optical-shaping methods. The present work excludes anisotropic deformations in Ag-As-S, which has been ascribed to photo-electro-ionic migration [9].

2. Classification

Several kinds of photoinduced polarization-dependent deformations are known to exist in covalent chalcogenide glasses such as As-S(Se). The phenomena may be classified, as listed in Table 1, into the four according to spot size of excitation light and persistency of deformations. The spot size can be smaller or larger than a sample lateral dimension. If the spot size is smaller, light-intensity gradient [10-12] and/or scattered light from the spot to periphery [9] can be responsible for deformations. If it is larger, such effects become very weak, and uniform-intensity illumination takes place. On the other hand, the persistency can be *transitory* (temporal) or *memorable*, respectively, for phenomena appearing only during illumination or remaining after termination of illumination. The memorable, however, may be erased by annealing at glass-transition temperatures or illumination of unpolarized light.

Table 1. Anisotropic deformations produced in chalcogenide films with exposure to linearly polarized light. OM represents opto-mechanical, and italics denote newly reported phenomena in the present work.

Persistency \ Spot size	Small	Large
Transitory	OM effect	OM effect (Fig. 1)
Memorable	M-shape (Fig. 3)	*Monolayer OM effect* (Fig. 2) Scratch (Fig. 4) *Crack* (Fig. 5) U-shape and spiral (Fig. 6)

3. Opto-mechanical effect

A famous transitory deformation is the opto-mechanical effect discovered by Krecmer et al. [13,14]. The sample is a bilayer consisting of, e.g., a sub-millimeter Si_3N_4 cantilever and an As-S-Se film, which deflects in response to the direction of an electric field of linearly polarized light (Fig. 1). The perpendicular and parallel polarizations to the cantilever long side bend the chalcogenide film outward and inward. Note, however, that the polarization-dependent bending is smaller than a thermal expansion effect by 1/5 – 1/10 [12,14]. And, when

illumination is ceased, the cantilever recovers its initial shape.

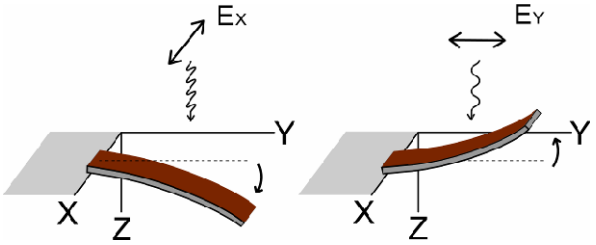

Fig. 1. A schematic illustration of the opto-mechanical effect. Thermal-expansion effects are neglected for clarity. The dark brown represents a chalcogenide film.

A role of light-spot sizes should be mentioned. In their work [13,14], the light spot is larger than cantilever lateral dimensions, providing uniform illumination. However, Asao and Tanaka have demonstrated that an opto-mechanical effect appears also when a light spot is much smaller (~1/10) than a cantilever dimension [12]. If the two phenomena occur under the same force remains to be studied.

4. Polarization-dependent deflection of As_2S_3 flakes

We have discovered a phenomenon, which can be termed as a *memorable* opto-mechanical effect, for As_2S_3 *monolayers* [15]. An As_2S_3 flake, with a thickness of ~10 μm and lateral dimensions of 150 and 550 μm, was obtained by peeling a deposited film off a substrate. (Unless otherwise specified, As_2S_3 films in the present study were prepared in the conventional way through vacuum evaporation on to glass substrates and annealing at ~180 °C in Ar atmosphere.) And, an end of the long side was pasted to a block as a cantilever.

Fig. 2 shows side views of the As_2S_3 cantilever. The left-hand side is fixed and the sample is exposed to laser light with uniform intensity which propagates downward in this image. Before illumination, the sample is straight (a). Upon illumination of the laser light of 2.3 eV and 400 mW/cm^2 with the electric field orthogonal to the sample long axis (normal to this sheet), the sample deflects to the propagating direction by ~15 μm/500 μm (b). This direction is consistent with that of the conventional opto-mechanical effect (Fig. 1). However, the deflection remains after termination of illumination (c), at least, a few minutes. Then, an exposure of parallel polarized light to the long axis (horizontal in this sheet) bends the flake upward (d), the direction also being consistent with the conventional one, but again being memorized. These deflections can be repeated, at least, several times. Note that actual deflections occur in horizontal planes, so that gravity effects can be neglected.

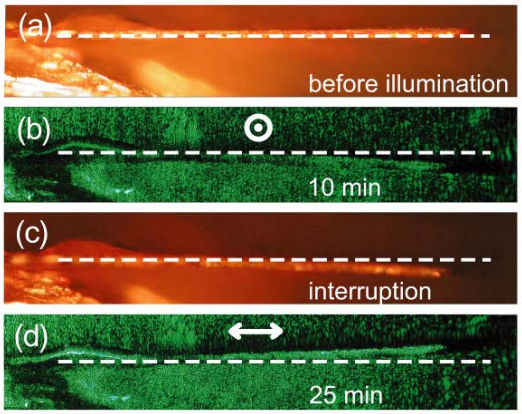

Fig. 2. Polarization-dependent deflection of an As_2S_3 cantilever. Red (a and c) and green (b and d) images are taken after and under excitation light, which propagates downward in these photographs with the polarization direction indicated. The horizontal dashes represent the initial state, and the times start from the beginning of the fist exposure.

A bending mechanism is speculative. The penetration depth α^{-1} of 2.3 eV light to As_2S_3 is ~50 μm ($\alpha \approx 200$ cm^{-1} and $n \approx 2.7$ at $\hbar\omega = 2.3$ eV), being much larger than the film thickness of ~10 μm. Accordingly, we may neglect penetration-depth effects. In addition, the polarization-dependent and persistent deflection excludes some effects arising from thermal strain and expansion, which are known to affect the conventional opto-mechanical effect [12-14]. Alternatively, the persistent deflection implies some role of stable force and material flow, which will be discussed in Section 8.

5. Anisotropic M-shaped deformation and scratch deformation

At least, two memorable anisotropic deformations are known to be produced by illumination of linearly polarized light.

One appears when a sample is exposed to a focused light spot with a diameter of 5-10 μm. For As_2S_3 films, Saliminia et al. have discovered an anisotropic deformation [10], which is M-shaped in the direction parallel to the electric field, while in the orthogonal direction the cross section appears as a simple concave (Fig. 3). A circular light-intensity distribution and a linearly polarized field seem to govern the deformation shape. Tanaka and Asao propose that this deformation occurs through a photo-electro-atomic process; *i.e.*, photoinduced anisotropic inter-molecular alignments and successive structural relaxation [11]. The anisotropic deformation changes to featureless patterns after prolonged illumination [11], which remains to be studied.

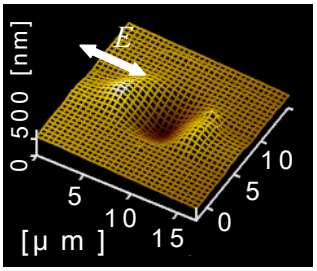

Fig. 3. An M-shaped deformation produced in an As_2S_3 film (2.3 μm thick) on glass with exposure to a focused (~5 μm) linearly-polarized light spot of 2.0 eV and ~2 mW for 2 h [11].

The other appears when scratched As-chalcogenide films are exposed to uniform illumination. Trunov et al. have discovered a photoinduced anisotropic scratch-deformation in films of $As_{20}Se_{80}$ [16] and As_2S_3 [17]. As illustrated in Fig. 4, when a crossed scratch on As-Se(S) films is exposed to linearly polarized light (a), parallel and perpendicular scratches to the electric field become smooth and prominent (b). In detail, a cross section of the perpendicular scratches appears to be M (or U) shaped with both sides lifting up. The anisotropic behavior is contrastive to isotropic surface smoothing, which seems to be a manifestation of photoinduced fluidity [18,19].

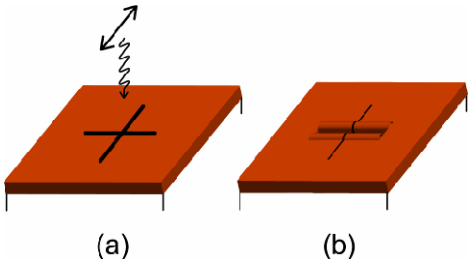

Fig. 4. Photoinduced smoothing and widening of scratches in parallel and perpendicular to the electric field of light.

6. Anisotropic crack deformation in As_2S_3

We have discovered that a crack in As_2S_3 films offers anisotropic responses to illumination of linearly polarized light [15]. Fig. 5 shows a typical result obtained in an As_2S_3 film (~4 μm thick), which contains an accidentally produced T-shaped crack (a), upon exposure to linearly polarized 2.3 eV light with ~1.5 W/cm^2. The laser light is unfocussed, and accordingly, the T crack is uniformly illuminated.

We see in the figure a prominently anisotropic response. A crack perpendicular (horizontal in these images) to the electric filed of light becomes wider, in clear contrast to a parallel crack, which is mostly intact. Surprisingly, after illumination of ~4 h (c), the crack grows to a width of ~50 μm. In the gap region, no As_2S_3 layer exists. We also see big banks on both sides of the crack. The cross-sectional views, obtained using an AFM, manifest that the volumes of the bank and the crack are comparable, which suggests mass transfer from the crack to the side banks.

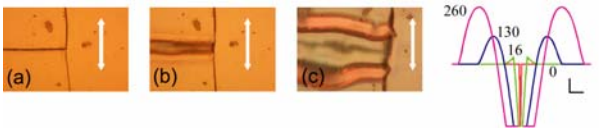

Fig. 5. Crack responses (interference optical images) in an As_2S_3 film on a slide glass upon exposure to linearly-polarized green light at exposure times of (a) 0, (b) 0.5, and (c) 4 h. The arrows in the images represent the electric-field direction, and its lengths are scaled to 50 μm. The right cross-sections show a growth of the horizontal crack at exposure times indicated (min), in which the horizontal and vertical lengths of "L" represent 10 and 1 μm.

Four features are worth mentioning for the anisotropic crack response. First, it occurred irrespective of substrate materials, slide glass and Si wafer, which have different optical and electrical properties. Second is a spectral dependence, which was examined using a 4.4 μm-thick film and lasers emitting photons of 1.8, 2.0, 2.3, and 2.8 eV. Here, 2.3 eV light ($\alpha^{-1} \approx 50$ μm) was the most efficient (in consistent with that in Fig. 8). Third is a sample-thickness dependence, which was examined using the 2.3 eV light and samples with thicknesses of 0.3, 4.4, 10, and 200 μm, the last being a polished bulk layer. Among these, the 10μm-thick As_2S_3 film gave the biggest change. The bulk flake also showed a crack widening with a smaller degree. The last feature is that an a-Se film with a thickness of 1.5 μm has undergone some changes upon exposure to linearly polarized 1.8 eV light, while the anisotropy is unclear. This observation may be consistent with the flake deformation [8], described in Section 7.

The crack deformation resembles the scratch deformation [16,17] in the anisotropic responses to the electric field, which may imply similar mechanisms. However, for the crack growth, it is difficult to envisage mass transport and atomic interaction between both sides of a crack. Another difference can be pointed out for scratches and cracks *parallel* to the electric field. The scratch becomes smooth and fades away (Fig. 4), but no such a change occurs in the crack (Fig. 5).

7. Anisotropic deformation of As_2S_3 flakes

As reported in a recent work [8], As_2S_3 flakes *free from (non-sticking to) substrates* deform anisotropically upon illumination of linearly polarized light. Fig. 6 shows a typical result obtained for a circular film with a thickness

and diameter of ~1 μm and 100 μm. The disk is put on silicone grease (a), *i.e.* free, and exposed to unfocussed 2.3 eV laser light with an intensity of 40 mW. We see that, at first (b, 10 min), the circular edges in the direction parallel to the electric field of light curl upward, *i.e.*, toward the light source. The cross section obtained from horizontal sides appears as "U". Then, the sample elongates in perpendicular to the electric field. At 80 min (c), it spirals, and ultimately it becomes as a thread-like (d).

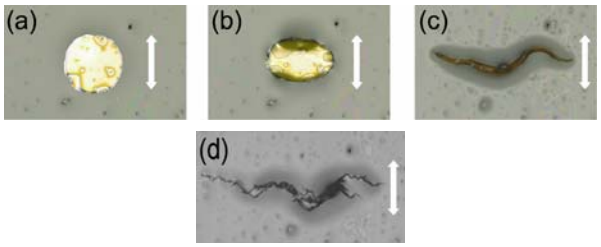

Fig. 6. Deformation of an As_2S_3 flake on silicone grease induced by linearly-polarized 2.3 eV laser light at exposure times of (a) 0, (b) 10, (c) 80, and (d) 1100 min. The light propagates toward the sample from our side. The arrow length is scaled to 100 μm, and the direction represents the electric field. Slight interference colors (0 and 10 min) reflect thin grease, and gray regions around the deformed sample (prominent at 80 and 1100 min) are caused by grease curvature arising from surface tension.

Samples fixed as cantilevers show interesting responses. As shown in Fig. 7, two As_2S_3 flakes with a thickness of ~3 μm and lateral dimensions of 100 – 200 μm have been pasted to a glass edge using grease, and exposed to the laser light (2.3 eV and 40 mW) with an electric field vertical in these images. We see that the deformations appear to be contrastive. The upper sample is U-shaped (b, 30 min), elongates, and screwing (c, 120 min), which are qualitatively consistent with the deformation of the sample on grease (Fig. 6). The sample also bends downward, the direction reflecting the gravity. On the other hand, the lower sample just bends *upward*, which is consistent with Fig. 2(d) and Fig. 6(b). It is suggested in Section 8 that these bends occur through optical force, photoinduced birefringence, and photoinduced fluidity [18,19].

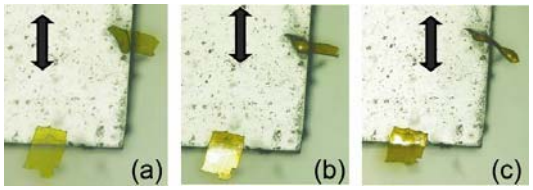

Fig. 7. Deformations of two As_2S_3 flakes fixed at a glass edge at exposures of (a) 0, (b) 0.5, and (c) 2 h. The arrows show the electric-field direction, and its length is scaled to 200 μm.

Effects of different exposure arrangements have been investigated using the 2.3 eV laser and As_2S_3 flakes with a few micron-meter thickness put on grease or frosted glass. One is the dependence on the angle of light incidence. Obliquely incident light, e.g. with an incident angle of 45°, having linear *s*- and *p*-polarization has produced the U-shape deformation and elongation perpendicular to the electric filed. On the other hand, if the light is incident normally to an As_2S_3 flake through a substrate, an inverse U-shape deformation and perpendicular elongation have occurred. The other is an effect induced by normally-incident circularly-polarized light. It has produced some shrinkage with no elongation, which can be regarded as a circularly-symmetric U shape.

Spectral dependence of quantum efficiency has been evaluated using several lasers and two As_2S_3 films with different thicknesses. The efficiency is defined as an inverse of the photon number which induces a fixed deformation, *i.e.*, a projected length reduction of 2% (reflecting the U shape) in the direction parallel to the electric field. We see in Fig. 8 a maximal efficiency at 2.0 – 2.4 eV and decreases on both sides. The low-energy decrease is probably due to a lack of photo-electronic excitation energy. And, the high-energy feature seems to reflect a penetration-depth effect, which is consistent with a lower efficiency in the thicker film.

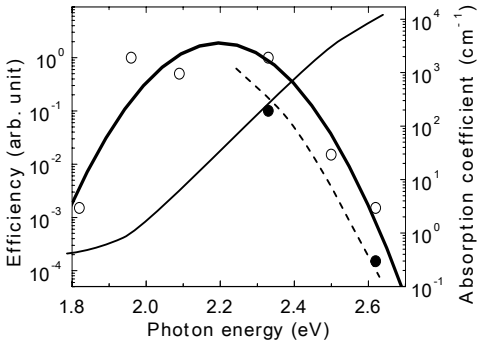

Fig. 8. Spectral dependence of a deformation efficiency for circular As_2S_3 films, with a diameter of ~100 μm and thicknesses of 1 (○) and 7 (●) μm, on grease. As a reference, the absorption spectrum is plotted, from which the light-penetration depth can be estimated. Maximal efficiency is normalized to unity.

A few-micron thick Se films have provided two kinds of deformations, as shown in Fig. 9, which are clearly different from that (Fig. 6) in As_2S_3. A light source employed is a semiconductor laser emitting linearly polarized light of 1.8 eV ($\alpha \approx 700$ cm^{-1} and $n \approx 2.7$), the photon energy being slightly less than the optical gap of ~1.9 eV, and an intensity of 20 mW. Se flakes on grease have elongated *parallel* to the direction of light polarization (upper sequence). Or, the flake tends to align parallel to the propagation direction of light. On the other

hand, a tiny (~5 μm) circular Se flake on frosted glass has exhibited just an isotropic shrinkage, which may appear from elongation along the light propagation direction (cylindrically isotropic U deformation). Se is stickier than As_2S_3, reflecting the low glass-transition temperature, which may cause these two behaviors.

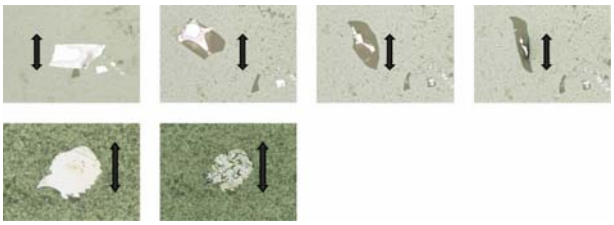

Fig. 9. Deformations of Se flakes with a thickness of ~1.5 μm on grease (upper) and frosted glass (lower) induced by 1.8 eV light. Exposure times are 0, 8, 27, 46 h for the upper sequence, and 0 and 20 h for the lower. The arrows represent the electric-field direction, and the lengths are scaled to 10 μm in the upper and 5 μm in the lower.

8. Optical force model

A common feature to these phenomena is the anisotropic U-shape deformation, where the electric field directs as if it were horizontal on this U character. Namely, we see Figs. 6 and 7 that the initial deformation of As_2S_3 flakes appears to be actually U-shaped along the light polarization. On the other hand, the edge of scratches (Fig. 4) and cracks (Fig. 5) appears in cross sections as ⌋⌊, being lifted up as L, which can be regarded as a left half of "U". For the bilayer and monolayer opto-mechanical effects (Figs. 2 and 3), the electric field along the long cantilever dimension deflects the sample toward a light source (opposite to a propagation direction), which can be regarded also as wide Us. We here propose that all these U deformations occur through photoinduced fluidity, photoinduced birefringence, and optical force.

The photoinduced fluidity is known to exist in covalent chalcogenide glasses such as As_2S_3 [18,19]. Upon (sub-)bandgap illumination at room temperature, the fluidity increases to $\sim 10^{-12}$ P^{-1}, which is nearly equal to the value thermally induced at around the glass-transition temperature. By contrast, several observations such as dependence upon illuminating temperature suggest that the photoinduced fluidity occurs non-thermally through a photo-electro-structural process, the atomic picture being speculative.

The photoinduced birefringence is also known to exist in chalcogenide glasses [3,20]. In covalent chalcogenide glasses, the birefringence is *negative*, i.e. $n(//) - n(+) < 0$ [21], where $n(//)$ and $n(+)$ are the refractive indices parallel and perpendicular to the electric field of excitation light. Fritzsche has ascribed this negative birefringence to selective photo-electronic excitation of anisotropic elements, which align parallel to the light polarization, and successive isotropic thermal relaxation [22]. Hence, the number of elements parallel to the light polarization reduces. However, atomic structures of the anisotropic element remain controversial [20].

It is known that several kinds of optical forces appear in small dielectrics, atoms, and so forth. The most famous, which is polarization-independent, may be the gradient force, appearing around focused light spots having intensity gradients. The force is widely employed in laser tweezers [23]. Radiation pressure, arising from photon momentum, is utilized for laser cooling and trapping of atoms and ions [24]. On the other hand, optical torque can appear when birefringent or non-spherical particles are irradiated by (un-)polarized light [25-30]. However, the angular direction and magnitude of generated torque depend upon many factors such as refractive index, birefringence, shape, and size of a particle [30]. And, to the best of the authors' knowledge, the optical torque for high refractive-index birefringent disks, which correspond to illuminated As_2S_3, has not been calculated. Hence, we summarize qualitative results probably pertinent to the present observations. Cheng et al. [27] demonstrate that micro-disks, irrespective of birefringence, tend to align with an edge-on orientation, *i.e.* the disk normal axis being perpendicular to the light propagation direction (Fig. 10(b)). On the other hand, Liu et al. [29] demonstrate using an exact calculation that spherical uniaxially-birefringent particles can orient so that the fast axis (the direction having smaller refractive index) align parallel to the electric field. Appendix will provide another simpler view.

Taking the photoinduced fluidity, photoinduced birefringence, and optical torque into account, we can draw a scenario for the U-shape deformation as illustrated in Fig. 10. When linearly-polarized bandgap light with E_x illuminates an As_2S_3 disk (a), the negative birefringence ($n_x < n_y = n_z$) appears. Then, the disk shape and this uniaxial refractive index seem to generate an optical torque which rotates the disk to the *y*-*z* plane (b) [27,29]. Actually, tiny (~10 μm) flakes of glassy As_2S_3 and also crystalline As_2S_3 (orpiment), the latter being known to be a negative birefringent material, on grease have aligned in such a manner [8]. However, for larger disks of ~100 μm put on grease or frosted glass, such rotation is mechanically difficult. Instead, the photoinduced fluidity makes possible upward-bending of the edges on the *x* axis (c). This deformation is assumed to be the U shape in Fig. 6. If the light is circularly polarized, cylindrically isotropic U-shape deformation occurs, which appears as an isotropic shrinkage in top views, in consistent with the observations. This model is consistent also with exposure-time dependences of birefringence and optical torque [8]. It should be underlined that the motive force of deformation in the present model is optical, not atomic as have commonly been proposed.

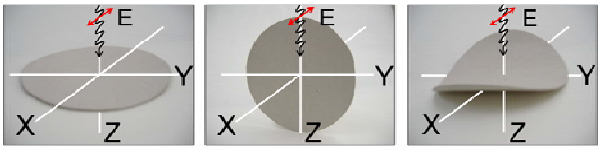

Fig. 10. A schematic model for photoinduced anisotropic deformations in an As_2S_3 disk. (a) The disk initially lies in the x-y plane, and linearly polarized light with the electric field in the x direction propagates downward along the z direction. The photoinduced birefringence makes the refractive index n_x, which corresponds to n(///), smaller. (b) The optical torque arising from the disk shape and the anisotropic refractive index tends to rotate the disk to the y-z plane. (c) However, for the disk on a substrate, the rotation is replaced by the edge bending with photoinduced fluidity.

The present idea can explain other deformations. The U-shape deformation of an As_2S_3 flake at the glass edge in Fig. 7 can be understood similarly. For the bilayer (Fig. 2) and monolayer (Fig. 3) opto-mechanical effects, the inward deflections when the electric field aligns along the long axis of a cantilever can be regarded as the U deformation. And, at the edge of cracks and scratches such bending can occur, which will appear as L shaped (upward bending) as in Figs. 4 and 5. The featureless deformation, which appears after the anisotropic M-shape deformation, upon focused linearly polarized bandgap illumination [11], may be influenced by the optical torque.

It seems straightforward to extend the present idea to other materials. The different deformations in Se can be ascribed to no appreciable photoinduced birefringence at room temperature [20], due to a low glass-transition temperature of ~30°C. In specific, the elongation along the electric field (Fig. 9(a)) may be consistent with the alignment demonstrated for non-birefringent materials [28]. Anisotropic deformations in azo-polymers and etc. [3] may be understood in a similar way

Nevertheless, quantitative evaluations of the deformation by the optical torque remain to be studied. For instance, using existing models for particles and liquids [30,31], we may estimate the torque T very roughly at 10^{-16} N·m under a light intensity of 1 W. Then, using the photoinduced viscosity η of 10^{12} P [18,19], an exposure time t of 10^4 s, and the relevant sample dimension R and thickness W, we obtain a deformation D (~ $Tt/(RW\eta)$) of 10^{-13} m, which is smaller by 6 - 8 orders than the observation. Incorporation of other ideas such as nonlinear, microscopic, and/or resonance effects [32,33] may be needed. Or, the viscosity under bandgap illumination may be smaller (~10^3 P) and/or anisotropic.

9. Remaining problems

In addition, we confront, at least, with three problems. One concerns with the phenomena which imply material flow orthogonal to the electric field. These include the downward deflection in the opto-mechanical effects of bilayer (Fig. 2, left) and monolayer (Fig. 3(b)) samples, the smoothing of parallel scratches to the electric field (Fig. 4), and the orthogonal elongation of As_2S_3 flakes (Fig. 6). Relevant motive force may arise also from the optical torque [30,31], which is consistent with a correlated decrease in optical torque with the elongation [8]. Otherwise, it may arise from the optical pressure which is produced by scattered light at incident surfaces [8,9]. The scattering occurs more strongly in directions perpendicular to the electric field [34]. This idea is consistent with the unchanging *crack* parallel to the electric field (Fig. 5), since the scattered light becomes much weaker when propagating a crack gap. The other problem is the different deformations upon different light illuminations such as oblique and backward incidence. To understand the features, we need to calculate optical torque for high-refractive (~2.6) and birefringent disks, which seems to be difficult. And, the most fascinating problem is the flake spiraling (Fig. 6(c)), which may be related with photoinduced optical rotatory [20,35].

10. Conclusions

It has been demonstrated that the chalcogenide glass such as As_2S_3 exhibits several kinds of macroscopic anisotropic deformations upon illumination of linearly-polarized bandgap light. Many of these deformations can be understood qualitatively through photoinduced birefringence, optical torque, and photoinduced fluidity. The birefringence and the torque provide an anisotropic stress, and the fluidity transforms the stress to persistent deformations. This new type of light-glass interaction reveals a tempting aspect of covalent chalcogenide glasses, which may be promising in optical glass-shaping applications.

Acknowledgements

The authors thank Mr. H. Asao for his skillful experiments, Dr. M. Trunov for private correspondences, and Keyence Corporation for use of a digital microscope VHX-600.

Appendix

The optical force has been calculated using ray tracing [25,26] and rigorous light-wave [27-31] formalisms, respectively, for large and arbitral-size particles in comparison with the wavelength λ of light. However, the scattering calculations [26-30] are complicated, and unified pictures are difficult to obtain.

We here outline a rough energetic view which can predict a stable shape of a deformable material with a fixed volume in a light field. For linearly-polarized light with E_x and H_y propagating to the z direction (Fig. 10), the

electromagnetic energy u including the material can be written down as;

$$u = (1/2)\int \varepsilon_x \left| E_x \right|^2 dV + (1/2)\int \mu_y \left| H_y \right|^2 dV,$$

where the integral is performed for a cross section of light and an appropriate thickness covering the sample. If the material is nonmagnetic, the second term becomes to be independent of the material shape, and we can neglect it. And, for a transparent material at an optical frequency, $\varepsilon_x = n_x^2 \varepsilon_0$. On the other hand, $E_x = E_0 - E_1$ in the sample, where E_0 is the incident field and E_1 is the depolarization field, which reflect the sample shape [36,37]. If the sample dimension along the x direction L_x is $L_x >> \lambda$, $E_1 \approx 0$, and $E_x \approx E_0$. On the other hand, if $L_x \leq \lambda$ (Rayleigh limit), under neglecting optical interference we may follow a result for static fields [36,37], obtaining $E_0 > E_1 > 0$. Accordingly, E_x tends to decrease with a decrease in L_x. Namely, u becomes smaller in a thinner material in the x direction. For instance, the material may be a flat disk, the normal directing to the x axis [27] as that in Fig. 10(b), or the material may be a long rod aligning along the y or z directions [30]. In addition, if the material is uniaxially negative birefringent, the optical axis tends to align along the x direction [30], which can decrease ε_x and u. We can approximate the deformation observed in As_2S_3 by these rules. It seems straightforward to extend the present notion to orientation problems of rigid materials (such as c-As_2S_3) and to laser tweezers using focused light.

References

[1] K. Tanaka, A. Saitoh, N. Terakado, J. Optoelectron. Adv. Mater. **8,** 2059 (2006).
[2] E. Vateva, J. Optoelectron. Adv. Mater. **9,** 3108 (2007).
[3] V. M. Kryshenik, M. L. Trunov, V. P. Ivanitsky, J. Optoelectron. Adv. Mater. **9,** 1949 (2007).
[4] H. Ishitobi, M. Tanabe, Z. Sekkat, S. Kawata, Opt. Exp. **15,** 652 (2007).
[5] S. Kobatake, S. Takami, H. Muto, T. Ishikawa, M. Irie, Nature **446,** 778 (2007).
[6] J. Ilinytskyi, M. Saphiannikova, D. Neher, Condens. Matter Phys. **9,** 87 (2006).
[7] J. Hegedus, K. Kohary, S. Kugler, J. Phys. Chem. Solids **68,** 1069 (2007).
[8] K. Tanaka, APEX **1,** ?? (2008).
[9] T. Gotoh, K. Tanaka, J. Appl. Phys. **89,** 4703 (2001).
[10] A. Saliminia, T. V. Galstian, A. Villeneuve, Phys. Rev. Lett. **85,** 4112 (2000).
[11] K. Tanaka, H. Asao, Jpn. J. Appl. Phys. **45,** 1668 (2006).
[12] H. Asao, K. Tanaka, J. Appl. Phys. **102,** 43508 (2007).
[13] P. Krecmer, A. M. Moulin, R.J. Stephenson, T. Rayment, M. E. Welland, S.R. Elliott, Science **277,** 1799 (1997).
[14] M. Stuchlik, S. R. Elliott, J. Non-Cryst. Solids **353,** 250 (2007).
[15] The phenomena were discovered in November 2006 – February 2007 by H. Asao, a master-course student of our group.
[16] M. L. Trunov, A. S. Bilanich, S. N. Dub, J. Non-Cryst. Solids **353,** 1904 (2007).
[17] M. L. Trunov, JETP Lett. **86,** 313 (2007).
[18] H Hisakuni, K. Tanaka, Science **270,** 974 (1995).
[19] K. Tanaka, C. R. Chimie **5,** 805 (2002).
[20] K. Tanaka, Handbook of Advanced Electronic and Photonic Materials and Devices, edited by H. S. Nalwa (Academic Press, 2001) Vol. 5, Chap. 4.
[21] V. G. Zhdanov, V. K. Malinovsky, Sov. Tech. Phys. Lett. **3,** 387 (1977).
[22] H. Fritzsche, J. Non-Cryst. Solids **164/166**, 1169 (1993).
[23] H. Ukita, Micromechanical Photonics (Springer, 2006).
[24] H. J. Metcalf, P. Van der Straten, Laser Cooling and Trapping (Springer, 1999).
[25] R. A. Beth, Phys. Rev. **50,** 115 (1936).
[26] R. C. Gauthier, J. Opt. Soc. Am. B **14,** 3323 (1997).
[27] Z. Cheng, P. M. Chaikin, T. G. Mason, Phys. Rev. Lett. **89,** 108303 (2002).
[28] S. Bayoudh, T. A. Nieminen, N. R. Heckenberg, H. Rubinsztein-Dunlop, J. Mod. Opt. **50,** 1581 (2003).
[29] M. Liu, N. Ji, Z. Lin, S. T. Chui, Phys. Rev. E **72,** 56610 (2005).
[30] W. Singer, T. A. Nieminen, U. J. Gibson, N. R. Heckenberg, H. Rubinsztein-Dunlop, Phys. Rev. E **73,** 21911 (2006).
[31] A. Yu. Savchenko, N. V. Tabiryan, B. Ya. Zel'dovich, Phys. Rev. B **56,** 4773 (1997).
[32] Thai. V. Truong, Y. R. Shen, Phys. Rev. Lett. **99,** 187802 (2007).
[33] A. T. Ohta, P. –Y. Chiou, H. L. Phan, S. W. Sherwood, J. M. Yang, A. N. K. Lau, H. –Y. Hsu, A. Jamshida, M. C. Wu, IEEE J. Selected Topics Quant. Electron. **13,** 235 (2007).
[34] H. C. van de Hulst, Light Scattering by Small Particles (Dover, 1981) Chap. 7.
[35] J. Hajto, P. J. S. Ewen, Phys. Stat. Sol. (a) **54,** 385 (1979).
[36] R. Schiffer, K. O. Thielheim, J. Appl. Phys. **50,** 2476 (1979).
[37] C. Kittel, Introduction to Solid State Physics, 8th ed. (John Wiley & Sons, 2005) Chap. 16.

*Corresponding author: keiji@eng.hokudai.ac.jp